THE JOURNAL OF BIOLOGICAL CHEMISTRY VOL. 284, NO. 18, pp. 12480–12490, May 1, 2009

Reciprocal Intramolecular Interactions of Tomosyn Control Its Inhibitory Activity on SNARE Complex Formation*[S]

Received for publication, September 16, 2008, and in revised form, February 27, 2009 Published, JBC Papers in Press, March 3, 2009, DOI 10.1074/jbc.M807182200

Yasunori Yamamoto[‡], Sumiko Mochida[§], Takao Kurooka[‡], and Toshiaki Sakisaka[‡1]

From the [‡]Division of Membrane Dynamics, Department of Physiology and Cell Biology, Kobe University Graduate School of Medicine, Kobe 650-0017 and the [§]Department of Physiology, Tokyo Medical University, Tokyo 160-8402, Japan

Neurotransmitter release from presynaptic nerve terminals is regulated by SNARE complex-mediated synaptic vesicle fusion. Tomosyn, a negative regulator of neurotransmitter release, which is composed of N-terminal WD40 repeats, a tail domain, and a C-terminal VAMP-like domain, is known to inhibit SNARE complex formation by sequestering target SNAREs (t-SNAREs) upon interaction of its C-terminal VAMP-like domain with t-SNAREs. However, it remains unclear how the inhibitory activity of tomosyn is regulated. Here we show that the tail domain functions as a regulator of the inhibitory activity of tomosyn through intramolecular interactions. The binding of the tail domain to the C-terminal VAMP-like domain interfered with the interaction of the C-terminal VAMP-like domain with t-SNAREs, and thereby repressed the inhibitory activity of tomosyn on the SNARE complex formation. The repressed inhibitory activity of tomosyn was restored by the binding of the tail domain to the N-terminal WD40 repeats. These results indicate that the probable conformational change of tomosyn mediated by the intramolecular interactions of the tail domain controls its inhibitory activity on the SNARE complex formation, leading to a regulated inhibition of neurotransmitter release.

Synaptic vesicles are transported to the presynaptic plasma membrane where Ca^{2+} channels are located. Depolarization induces Ca^{2+} influx into the cytosol of nerve terminals through the Ca^{2+} channels, and this Ca^{2+} influx initiates the fusion of the vesicles with the plasma membrane, finally leading to exocytosis of neurotransmitters (1). Soluble *N*-ethylmaleimide-sensitive fusion protein attachment protein (SNAP)[2] receptors (SNAREs) are essential for synaptic vesicle exocytosis (2–5). Synaptic vesicles are endowed with vesicle-associated membrane protein 2 (VAMP-2) as a vesicular SNARE, whereas the presynaptic plasma membrane is endowed with syntaxin-1 and SNAP-25 as target SNAREs. VAMP-2 interacts with SNAP-25 and syntaxin-1 to form a stable SNARE complex (6–9). The formation of the SNARE complex then brings synaptic vesicles and the plasma membrane into close apposition, and provides the energy that drives the mixing of the two lipid bilayers (3–5, 9).

Tomosyn is a syntaxin-1-binding protein that we originally identified (10). Tomosyn contains N-terminal WD40 repeats, a tail domain, and a C-terminal domain homologous to VAMP-2. The C-terminal VAMP-like domain (VLD) of tomosyn acts as a SNARE domain that competes with VAMP-2. Indeed, a structural study of the VLD revealed that the VLD, syntaxin-1, and SNAP-25 assemble into a SNARE complex-like structure (referred to as tomosyn complex hereafter) (11). Tomosyn inhibits SNARE complex formation by sequestering t-SNAREs through the tomosyn complex formation, and thereby inhibits SNARE-dependent neurotransmitter release. The large N-terminal region of tomosyn shares similarity to the *Drosophila* tumor suppressor lethal giant larvae (Lgl), the mammalian homologues M-Lgl1 and M-Lgl2, and yeast proteins Sro7p and Sro77p (12, 13). Consistent with the function of tomosyn, Lgl family members play an important role in polarized exocytosis by regulating SNARE function on the plasma membrane in yeast and epithelial cells (12, 13). However, only tomosyn, Sro7, and Sro77 have the tail domains and the VLDs, suggesting that their structural regulation is evolutionally conserved. Recently, the crystal structure of Sro7 was solved and revealed that the tail domain of Sro7 binds its WD40 repeats (14). Sec9, a yeast counterpart of SNAP-25, also binds the WD40 repeats of Sro7. This binding inhibits the SNARE complex formation and exocytosis by sequestering Sec9. In addition, binding of the tail domain to the WD40 repeats causes a conformational change of Sro7 and prevents the interaction of the WD40 repeats with Sec9, leading to regulation of the inhibitory activity of Sro7 on the SNARE complex formation (14). However, the solved structure of Sro7 lacks its VLD. Therefore, involvement of the activity of the VLD in the conformational change of Sro7 remains elusive.

Genetic studies in *Caenorhabditis elegans* showed that TOM-1, an ortholog of vertebrate tomosyn, inhibits the priming of synaptic vesicles, and that this priming is modulated by the balance between TOM-1 and UNC-13 (15, 16). Tomosyn was also shown to be involved in inhibition of the exocytosis of dense core granules in adrenal chromaffin cells and PC12 cells (17, 18). Thus, evidence is accumulating that tomosyn acts as a negative regulator for formation of the SNARE complex,

* This work was supported by Grants-in-aid for the National Project on Targeted Proteins Research Program (to T. S.), for Scientific Research C (to T. S.), for Scientific Research on Priority Areas-Elucidation of neural network function in the brain (to T. S. and S. M.), for Scientific Research B (to S. M.), and for the Global COE Program F11 (to T. S.) from the Ministry of Education, Culture, Sports, Science, and Technology, Japan.

[S] The on-line version of this article (available at http://www.jbc.org) contains supplemental Figs. S1–S6.

[1] To whom correspondence should be addressed. Tel.: 81-78-382-5727: Fax: 81-78-382-5419; E-mail: sakisaka@med.kobe-u.ac.jp.

[2] The abbreviations used are: SNAP, soluble *N*-ethylmaleimide-sensitive fusion protein attachment protein; SNARE, soluble *N*-ethylmaleimide-sensitive fusion protein attachment protein receptor; VAMP, vesicle-associated membrane protein; VLD, VAMP-like domain; EPSP, excitatory postsynaptic potential; SCG, superior cervical ganglion; Lgl, lethal giant larvae; aa, amino acid(s); MBP, maltose-binding protein; GST, glutathione *S*-transferase; mAb, monoclonal antibody; HA, hemagglutinin.

thereby inhibiting various vesicle fusion events. However, the precise molecular mechanism regulating the inhibitory action of tomosyn has yet to be elucidated.

In the present study, we show that the tail domain of tomosyn binds both the WD40 repeats and the VLD and functions as a regulator for the inhibitory activity of tomosyn on the SNARE complex formation. Our results indicate that the probable conformational change of tomosyn mediated by the intramolecular interactions of the tail domain serves for controlling the inhibitory activity of the VLD.

EXPERIMENTAL PROCEDURES

Expression and Purification of Recombinant Protein—Expression vectors for full-length rat m-tomosyn (1–1116 aa) and a large N-terminal fragment of rat m-tomosyn (tomosyn-N) (1–949 aa) were constructed in pFastBac1-MBP using standard molecular biology methods. The pFastBac1-MBP vector was constructed from a baculovirus transfer vector, pFastBac1 (Invitrogen), to express a fusion protein with N-terminal maltose-binding protein (MBP) (19). MBP-fused full-length tomosyn (MBP-tomosyn) and MBP-fused tomosyn-N (MBP-tomosyn-N) were expressed in Sf21 cells. A cDNA encoding the VLD (1031–1116 aa) of rat m-tomosyn and a cDNA encoding the tail domain and the VLD (933–1116 aa) of rat m-tomosyn were subcloned into the pMAL-C2 vector (New England Biolabs Inc.). MBP-fused VLD (MBP-VLD) and MBP-fused tail-VLD (MBP-tail-VLD) were expressed in *Escherichia coli*. MBP-tomosyn, MBP-tomosyn-N, MBP-VLD, and MBP-tail-VLD were purified with amylose resin in accordance with the manufacturers manual. MBP-VLD and MBP-tail-VLD were further purified using Mono-Q (GE Healthcare). For the expression of His_6-tagged tail-VLD (His-tail-VLD), and His_6-tagged VLD (His-VLD), the cDNAs of tail-VLD and VLD were subcloned into pRSET vector and pTrc vector, respectively. For the expression of the His_6-tagged tail domain (His-tail), a cDNA encoding the peptide encompassing the tail domain (933–1050 aa) was subcloned into pRSET vector. His-tail-VLD, His-VLD, and His-tail were expressed in *E. coli* and purified with TALON resin (Clontech). For the expression of GST-fused VLD (GST-VLD), GST-fused syntaxin-1 (GST-syntaxin-1), GST-fused SNAP-25 (GST-SNAP-25), and GST-fused VAMP-2 (GST-VAMP-2), cDNA of the VLD and cDNAs encoding the cytoplasmic domain of syntaxin-1 (1–265 aa), full-length SNAP-25 (1–206 aa), and the cytoplasmic domain of VAMP-2 (1–94 aa) were subcloned into pGEX vectors. GST-VLD, GST-syntaxin-1, GST-SNAP-25, and GST-VAMP-2 were expressed in *E. coli* and purified with glutathione-Sepharose 4B in accordance with the manufacturer's manual. To cut off the GST tags, GST-VLD and GST-SNAP-25 were digested with PreScission protease, and GST-syntaxin-1 and GST-VAMP-2 were digested with thrombin. The GST tag and PreScission protease were removed by glutathione-Sepharose 4B. The thrombin was removed by benzamidine-Sepharose. Syntaxin-1 was further purified using Mono-Q as previously described (20).

Synaptic Transmission between SCG Neurons—Postnatal day 7 Wistar ST rats were decapitated under diethyl ether anesthesia according to the guidelines of the Physiological Society of Japan. Isolated SCG neurons were maintained in culture for 5–6 weeks as described (21, 22). In brief, SCGs were dissected, desheathed, and incubated with collagenase (0.5 mg/ml; Worthington Biochemical) in L-15 (Invitrogen) at 37 °C for 10 min. Following enzyme digestion, semi-dissociated ganglia were triturated gently through small-pore glass pipettes until a cloudy suspension was observed. After washing by low speed centrifugation at 1,300 × *g* for 3 min, the collected cells were plated onto coverslips in plastic dishes (Corning; 35-mm diameter, approximately one ganglion per dish) containing a growth medium of 84% Eagle's minimal essential medium (Invitrogen), 10% fetal calf serum (Invitrogen), 5% horse serum (Invitrogen), 1% penicillin/streptomycin (Invitrogen), and 25 ng/ml nerve growth factor (2.5 S, grade II; Alomone Laboratories). The cells were maintained at 37 °C in a 95% air, 5% CO_2-humidified incubator and the medium was changed twice per week. Excitatory postsynaptic potential (EPSP) recording and injection of the recombinant proteins were performed as described previously (21, 22). Electrophysiological data collected using software written by the late L. Tauc (Centre National de la Recherche Scientifique, Gif-sur-Yvette, France) were analyzed with Origin (Microcal Software Inc.).

Assays for Tomosyn Complex Formation and SNARE Complex Formation—For tomosyn complex formation, syntaxin-1 and SNAP-25 were reacted in the presence or absence of MBP-VLD, MBP-tail-VLD, or MBP-tomosyn in Buffer A (20 mM Tris/HCl, pH 7.5, 150 mM NaCl, 1 mM EDTA, 1 mM dithiothreitol, and 0.5% Nonidet P-40) at 4 °C overnight. For SNARE complex formation, the samples were further reacted with VAMP-2 in Buffer A at room temperature for 60 min. The formed tomosyn complex and SNARE complex were detected by native PAGE as previously described (20). Briefly, the samples were suspended in a loading buffer (60 mM Tris/HCl, pH 6.8, and 10% glycerol), and then separated on 3% stacking (Tris/HCl, pH 6.7) and 9% separation gel (Tris/HCl, pH 8.8) in an identical manner as SDS-PAGE except that SDS was omitted from all buffers. The SNARE complex was also detected by SDS-PAGE as previously described (23). Briefly, the samples were solubilized in SDS sample buffer A (60 mM Tris/HCl, pH 6.8, 25 mM dithiothreitol, 20 mM EDTA, 5% glycerol, and 2% SDS) at room temperature for 10 min. Then the samples were subjected to SDS-PAGE, followed by immunoblotting with an anti-syntaxin-1 mAb (a generous gift from Dr. Masami Takahashi (Kitasato University, Kanagawa, Japan)).

Assays for Effects of the Tail Domain Binding on Tomosyn Complex Formation and SNARE Complex Formation—To examine the effect of the binding of the tail domain to the VLD on the tomosyn complex formation and the SNARE complex formation, 1 μM VLD and various concentrations of His-tail were preincubated, and then the mixtures of VLD and His-tail were incubated with 1 μM syntaxin-1 and 1 μM SNAP-25 for 60 min. For tomosyn complex formation, the samples were subjected to native PAGE followed by Coomassie Brilliant Blue staining. For SNARE complex formation, the samples were further incubated with 1 μM VAMP-2 for 60 min at 4 °C, and the samples were solubilized in SDS sample buffer A at room temperature for 10 min and subjected to SDS-PAGE followed by immunoblotting with the anti-syntaxin-1 mAb. To examine the effect of binding of the tail domain to the WD40 repeats on the

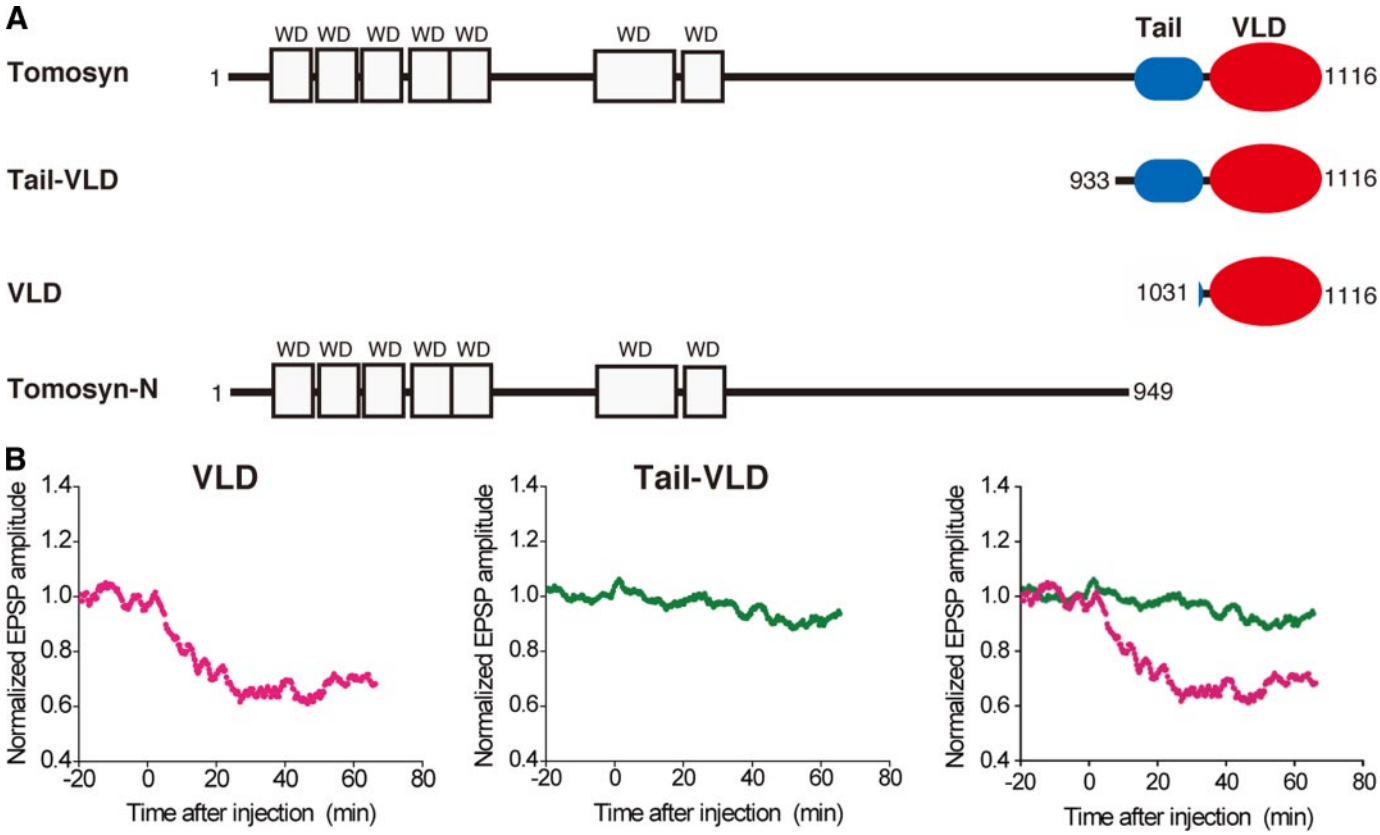

FIGURE 1. **Different inhibitory effects of tomosyn fragments on synaptic transmission between SCG neurons.** *A*, schematic structures of tomosyn and its truncated fragments used in this study. *B*, different effects of the tomosyn fragments on inhibition of synaptic transmission. MBP-fused VLD or MBP-fused tail-VLD was microinjected into the cell bodies of SCG neurons at time = 0 (100 μM in the pipette). EPSP amplitudes measured every 10 s were normalized and averaged (n = 5 or 6). The mean values smoothed by an eight-point moving average algorithm are plotted.

SNARE complex formation, 0.25 μM His-tail-VLD or 0.25 μM His-VLD were preincubated in the presence or absence of 0.5 μM MBP-tomosyn-N at 4 °C overnight. 0.25 μM Syntaxin-1 and 0.25 μM SNAP-25 were incubated with His-tail-VLD, His-VLD, the mixture of MBP-tomosyn-N and His-tail-VLD, or the mixture of MBP-tomosyn-N and His-VLD at 4 °C for 6 h, and then 0.25 μM VAMP-2 was added. After a subsequent 60-min incubation at room temperature, the samples were solubilized in SDS sample buffer A at room temperature for 10 min and subjected to SDS-PAGE, followed by immunoblotting with the anti-syntaxin-1 mAb.

Pull-down Assay for Binding of the Tail Domain to the VLD—For detection of the direct binding of His-tail to GST-VLD, 18 μmol of GST-VLD or GST alone was immobilized on 50 μl of glutathione-Sepharose 4B, and then incubated with 12 nmol of His-tail in Buffer B (20 mM Tris/HCl, pH 7.5, 20 mM NaCl, 1 mM EDTA, 1 mM dithiothreitol, and 0.5% Nonidet P-40) at 4 °C overnight. After the resins were extensively washed with Buffer B, the bound proteins were eluted by boiling in SDS sample buffer B (60 mM Tris/HCl, pH 6.7, 3% SDS, 2% 2-mercaptoethanol, and 5% glycerol) for 10 min. The samples were then subjected to SDS-PAGE, followed by immunoblotting with an anti-His mAb (Novagen).

Pull-down Assay for Binding of the Tail Domain to the N-terminal WD40 Repeats—For detection of the direct binding of His-tail to MBP-tomosyn-N, 150 pmol of MBP-tomosyn-N or MBP alone was immobilized on 50 μl of amylose resin, and then incubated with 405 pmol of His-tail-VLD or His-VLD in Buffer B at 4 °C overnight. After the resins were extensively washed with Buffer B, the bound proteins were eluted by boiling in SDS sample buffer B for 10 min. The samples were then subjected to SDS-PAGE, followed by immunoblotting with an anti-His polyclonal antibody (Santa Cruz). For quantitative analysis of the binding, 130 pmol of MBP-tomosyn-N were immobilized on 20 μl of amylose resin, and incubated with various concentrations of His-tail in Buffer B. After the resins were extensively washed with Buffer B, the bound proteins were eluted by boiling in SDS sample buffer B for 10 min and subjected to SDS-PAGE followed by Coomassie Brilliant Blue staining.

RESULTS

Different Inhibitory Effects of Tomosyn Fragments on Synaptic Transmission between SCG Neurons—Tomosyn is composed of N-terminal WD40 repeats, a tail domain, and a VAMP-like domain (VLD) (Fig. 1*A*). To examine how the activity of the VLD of tomosyn is regulated, we utilized a synapse formed between superior cervical ganglion (SCG) neurons in culture (24), because samples to be tested, such as proteins, can be easily introduced into the relatively large presynaptic cell bodies of SCG neurons by microinjection, allowing the effects on the stimulated release of acetylcholine to be accurately monitored by recording the EPSPs evoked by action potentials in the presynaptic neurons. The VLD is known to compete for VAMP-2 binding to syntaxin-1, leading to inhibition of SNARE

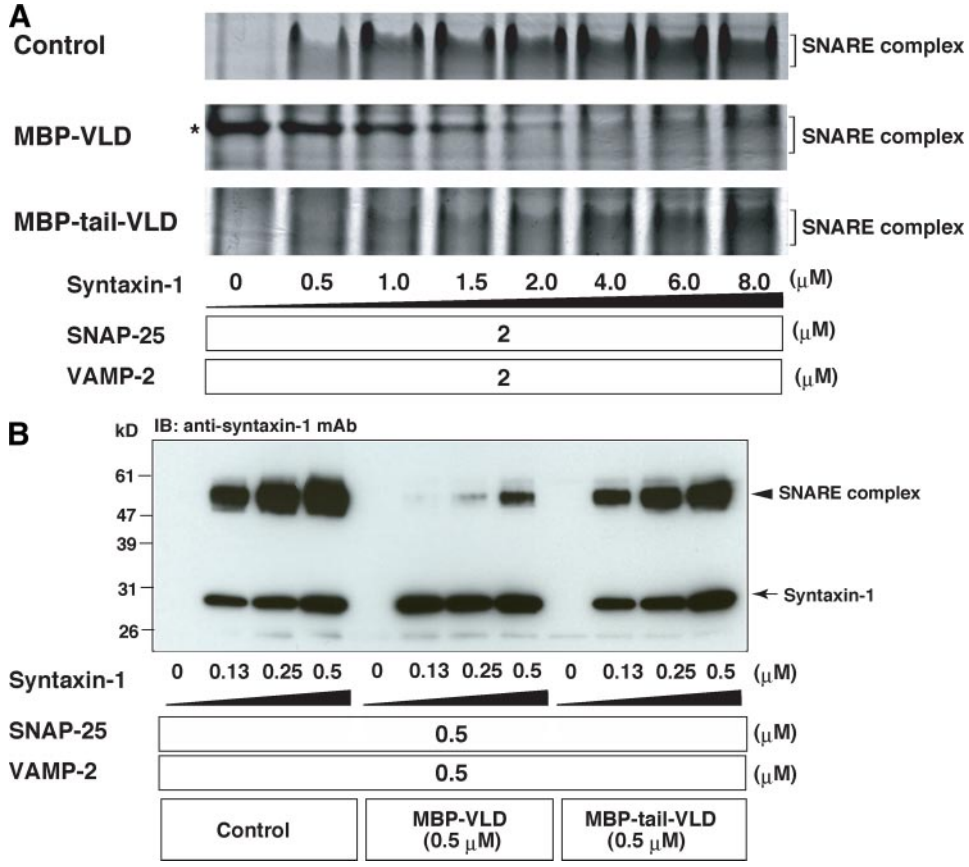

FIGURE 2. **Different inhibitory effects of tomosyn fragments on SNARE complex formation.** *A*, assessment of SNARE complex formation by native PAGE. Various concentrations of syntaxin-1, 2 μM SNAP-25, and 2 μM VAMP-2 were reacted in the presence or absence of 5 μM MBP-VLD or 5 μM MBP-tail-VLD. The samples were separated on 9% non-denaturing gel, followed by Coomassie Brilliant Blue staining. *Asterisk* shows the band of MBP-VLD. It is noted that the decrease of MBP-VLD in a dose-dependent manner of syntaxin-1 is due to tomosyn complex formation. *B*, assessment of the SDS-resistant SNARE complex formation. Various concentrations of syntaxin-1 were reacted with 0.5 μM SNAP-25 and 0.5 μM VAMP-2 in the presence or absence of 0.5 μM MBP-VLD or 0.5 μM MBP-tail-VLD. The samples were solubilized in SDS sample buffer at room temperature, subjected to SDS-PAGE followed by immunoblotting (*IB*) with the anti-syntaxin-1 mAb.

complex formation (11). Consistent with these facts, microinjection of an MBP-fused fragment encompassing the VLD (MBP-VLD) inhibited acetylcholine release (Fig. 1*B*). By contrast, microinjection of an MBP-fused fragment encompassing the tail domain and the VLD (MBP-tail-VLD) did not inhibit acetylcholine release.

Repression of the VLD-mediated Inhibition of the SNARE Complex Formation by the Tail Domain—To understand why MBP-tail-VLD did not inhibit neurotransmitter release, we examined the effect of the tail domain on the SNARE complex formation. SNAP-25, VAMP-2 lacking the transmembrane domain (referred to as VAMP-2 hereafter), and various concentrations of syntaxin-1 lacking the transmembrane domain (referred to as syntaxin-1 hereafter) were reacted in the presence or absence of MBP-VLD or MBP-tail-VLD. Then the samples were subjected to native PAGE as previously described (20), followed by Coomassie Brilliant Blue staining. In the control reaction, the SNARE complex was efficiently formed in a dose-dependent manner of syntaxin-1 (Fig. 2*A*). The SNARE complex in the control reaction began to form at 0.5 μM syntaxin-1. The reaction with MBP-VLD potently inhibited SNARE complex formation relative to the control reaction. The SNARE complex was not detected below 2.0 μM syntaxin-1. On the other hand, the reaction with MBP-tail-VLD moderately inhibited the formation of the SNARE complex relative to the control reaction. The amount of formed SNARE complex in the reaction with MBP-tail-VLD was less than that in the control reaction at all tested concentrations of syntaxin-1. However, the reaction with MBP-tail-VLD began to form the SNARE complex at 0.5 μM syntaxin-1. These results indicate that the ability of MBP-tail-VLD to inhibit SNARE complex formation is much weaker than that of MBP-VLD. Similar results were obtained by assessing SDS-resistant SNARE complex formation. Various concentrations of syntaxin-1 were reacted with SNAP-25 and VAMP-2 in the presence or absence of MBP-VLD or MBP-tail-VLD. The samples were solubilized in the SDS sample buffer at room temperature, and subjected to SDS-PAGE followed by immunoblotting with the anti-syntaxin-1 mAb. Consistent with the previous report that the SNARE complex is resistant to the SDS sample buffer at room temperature (23), 60-kDa immunoreactive bands indicative of the SNARE complex were detected. MBP-VLD inhibited SDS-resistant SNARE complex formation much more than MBP-tail-VLD (Fig. 2*B*). To validate these *in vitro* results, we examined inhibitory activities of Tail-VLD and VLD on the SNARE complex formation at a cell level. A vector to express HA-tagged VLD (HA-VLD) or FLAG-tagged Tail-VLD (FLAG-tail-VLD) was transfected into a neuroblastoma cell line, NG108 cells. After neuronal differentiation upon 1 mM dibutyryl cyclic AMP application, SNAP-25 was immunoprecipitated with the anti-SNAP-25 mAb, and the SNARE complex formation was assessed by co-immunoprecipitation of VAMP-2. HA-VLD and FLAG-tail-VLD were co-immunoprecipitated from the cells expressing HA-VLD and FLAG-tail-VLD, respectively (supplemental Fig. S1), indicating that tomosyn complexes were formed in the cells. VAMP-2 co-immunoprecipitated from cells expressing HA-VLD or FLAG-tail-VLD was less than that from the untransfected cells, indicating that tomosyn complexes inhibited SNARE complex formation. Importantly, HA-VLD decreased co-immunoprecipitation of VAMP-2 more potently than FLAG-tail-VLD. Taken together, all these results indicate that the ability of Tail-VLD to inhibit SNARE complex formation is much weaker

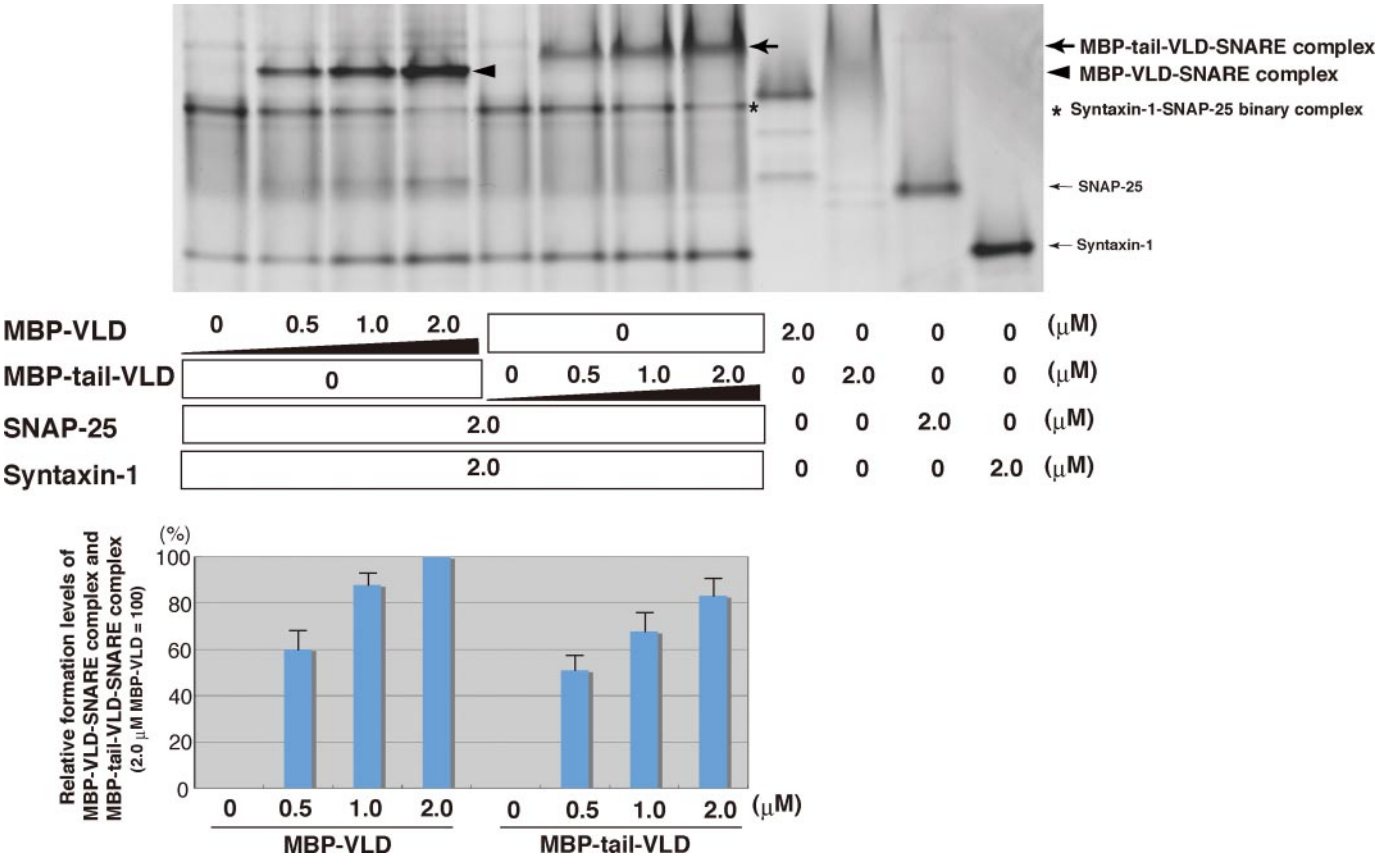

FIGURE 3. **Different effects of tomosyn fragments on tomosyn complex formation.** Various concentrations of MBP-VLD or MBP-tail-VLD were reacted with 2 μM syntaxin-1 and 2 μM SNAP-25. The samples were subjected to native PAGE followed by Coomassie Brilliant Blue staining. Quantification of the relative formation of tomosyn complexes (MBP-tail-VLD-SNARE complex and MBP-VLD-SNARE complex) is shown in the *lower panel*. The result shown is representative of three independent experiments. *Error bars* represent S.D.

than that of VLD, explaining why microinjection of MBP-tail-VLD into the SCG neuron did not inhibit neurotransmitter release.

Regulation of Tomosyn Complex Formation by the Tail Domain—We next examined the effect of the tail domain on tomosyn complex formation. Syntaxin-1 and SNAP-25 were reacted in the presence of various concentrations of MBP-VLD or MBP-tail-VLD. The samples were subjected to native PAGE followed by Coomassie Brilliant Blue staining, and the bands indicative of tomosyn complex (MBP-VLD-SNARE complex or MBP-tail-VLD SNARE complex) were quantified. MBP-VLD formed the tomosyn complex in a dose-dependent manner more efficiently than MBP-tail-VLD (Fig. 3). Next, we examined the time course of tomosyn complex formation by native PAGE. Syntaxin-1, SNAP-25, and MBP-VLD or MBP-tail-VLD were incubated for various periods of time at room temperature. Because native PAGE analysis does not allow the use of SDS sample buffer to terminate the reaction, we cannot exclude the possibility that the reaction proceeds during the native PAGE procedure. Indeed, some degree of tomosyn complex was formed without incubation at room temperature (supplemental Fig. S2). Under this condition, the tomosyn complex was still formed in a time-dependent manner. MBP-VLD-SNARE complex formation was saturated at 5 min incubation, whereas MBP-tail-VLD-SNARE complex formation was saturated at 60 min incubation. These results indicate that MBP-VLD forms the tomosyn complex more efficiently than MBP-tail-VLD. To further confirm the effects of MBP-VLD and MBP-tail-VLD on tomosyn complex formation, we titrated syntaxin-1 and examined the formation of the syntaxin-1-SNAP-25 binary complex by native PAGE. SNAP-25 and various concentrations of syntaxin-1 were reacted in the presence or absence of MBP-VLD or MBP-tail-VLD. The syntaxin-1-SNAP-25 binary complex was formed in the reaction with MBP-tail-VLD more efficiently than in that with MBP-VLD (supplemental Fig. S3*A*), indicating that MBP-VLD consumed the syntaxin-1-SNAP-25 binary complex for tomosyn complex formation more than MBP-tail-VLD. Taken together, all these results indicate that the activity of VLD to form the tomosyn complex is stronger than that of Tail-VLD, and suggest that the tail domain interferes with the activity of the VLD. Of note, the vague staining of MBP-tail-VLD alone on the native gel does not mean insufficient purity of the protein or loading smaller amounts of the protein. To confirm these results, the same samples were separated on an SDS-polyacrylamide gel (supplemental Fig. S3*B*). Given that migration of a protein on a native gel is influenced by its surface charge, such vague migration of MBP-tail-VLD may reflect a frequent change of the surface charge upon equilibration between association and dissociation of the tail domain to the VLD as discussed later. SNAP-25 migration on the native gel is much slower than syntaxin-1 although the molecular mass of SNAP-25 is lower than that of syntaxin-1.

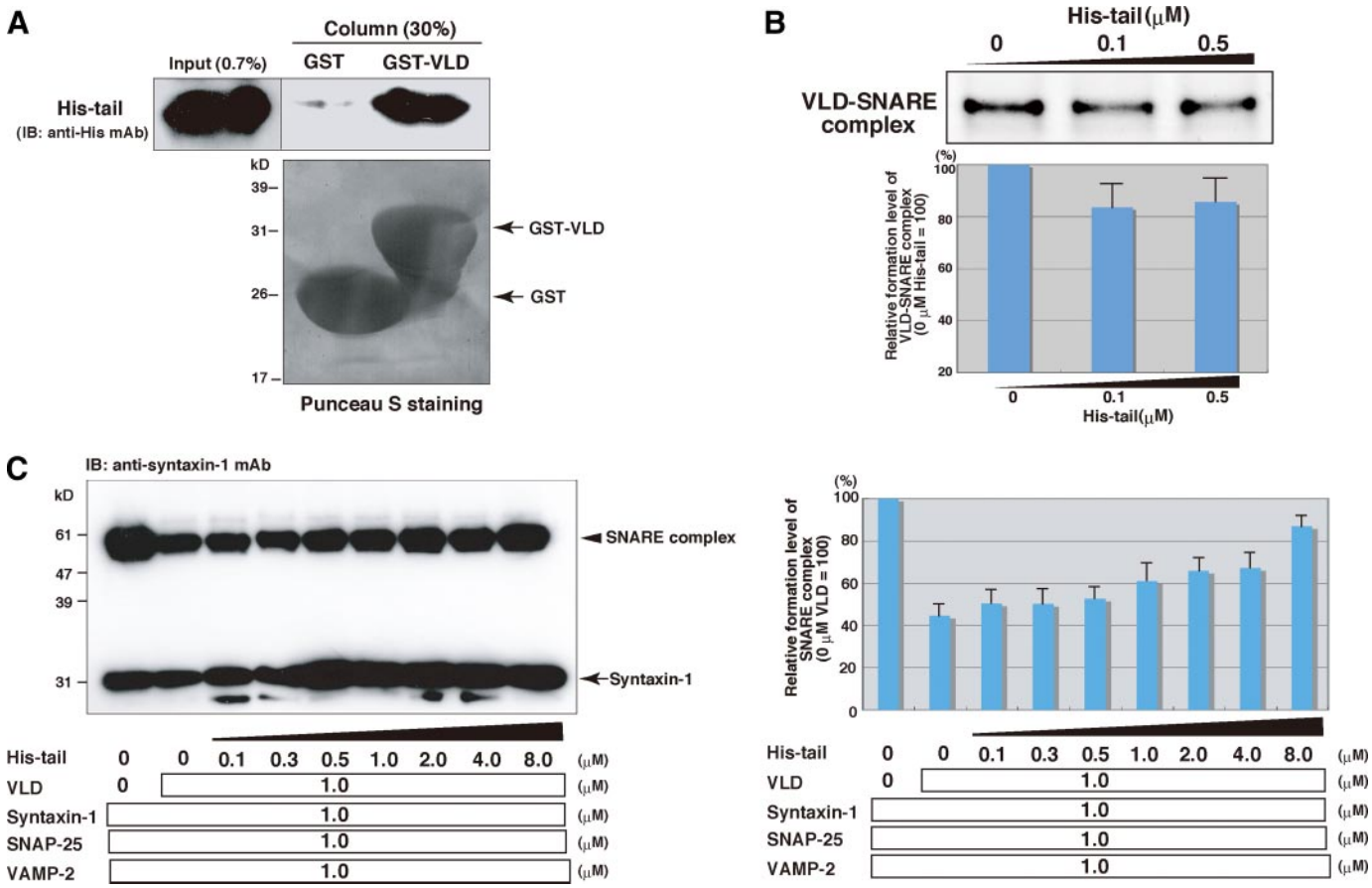

FIGURE 4. **Role of the binding of the tail domain to the VLD in inhibition of the SNARE complex formation.** *A*, direct binding of the tail domain to the VLD. GST-VLD or GST were immobilized on gluthathione-Sepharose and incubated with His-tail. After an extensive wash of resins, the bound proteins were eluted by boiling in SDS sample buffer. 0.7% of Input and 30% of the eluted proteins were subjected to SDS-PAGE, followed by immunoblotting (*IB*) with the anti-His mAb. *B*, decreased tomosyn complex formation upon binding of the tail domain to the VLD. 1 μM VLD was preincubated with various concentrations of His-tail, and then reacted with 1 μM syntaxin-1 and 1 μM SNAP-25. The samples were subjected to native PAGE followed by Coomassie Brilliant Blue staining. Quantification of the relative formation of the VLD-SNARE complex is shown in the *lower panel*. The result shown is representative of three independent experiments. *Error bars* represent S.D. *C*, loss of the inhibitory activity of the VLD upon direct binding of the tail domain to the VLD. 1 μM VLD was preincubated with various concentrations of His-tail, and then reacted with 1 μM syntaxin-1, 1 μM SNAP-25, and 1 μM VAMP-2. The samples were solubilized in the SDS sample buffer at room temperature for 10 min, and subjected to SDS-PAGE followed by immunoblotting with the anti-syntaxin-1 mAb. Quantification of the relative formation of the SNARE complex is shown in the *right panel*. The result shown is representative of three independent experiments. *Error bars* represent S.D.

These results indicate that syntaxin-1 is more negatively charged than SNAP-25 under the native PAGE conditions. These observations are also consistent with the previous report (20).

Role of the Binding of the Tail Domain to the VLD in Regulation of SNARE Complex Formation—The above results prompted us to examine whether the tail domain directly bound the VLD. GST or GST-fused VLD (GST-VLD) immobilized on glutathione-Sepharose was reacted with histidine-tagged peptide encompassing the tail domain (His-tail). After extensive wash of the resins, the bound proteins were eluted with the SDS sample buffer and then subjected to SDS-PAGE, followed by immunoblotting with the anti-His mAb. Specific binding of His-tail to GST-VLD was detected (Fig. 4*A*). These results indicate that the tail domain has an ability to bind the VLD. Consistent with these results, we observed co-immunoprecipitation of HA-tagged tail-VLD with FLAG-tagged tail-VLD but not that of HA-tagged VLD with FLAG-tagged VLD in HEK 293 cells (supplemental Fig. S4*A*). We next examined the functional role of the binding of the tail domain to the VLD in tomosyn complex formation by native PAGE. Syntaxin-1, SNAP-25, and VLD were reacted in the presence or absence of His-tail. His-tail decreased formation of the tomosyn complex (VLD-SNARE complex) (Fig. 4*B*). We further confirmed these observations by assessing the effect of the binding of the tail peptide to VLD on SNARE complex formation. Syntaxin-1, SNAP-25, and VAMP-2 were reacted in the presence of VLD and various concentrations of His-tail. The samples were solubilized in SDS sample buffer at room temperature, and then SNARE complex formation was examined by immunoblotting with the anti-syntaxin-1 mAb. His-tail increased the SNARE complex formation in a dose-dependent manner (Fig. 4*C*), indicating that binding of the tail domain to the VLD hinders the activity of the VLD to consume the binary complex for tomosyn complex formation. Collectively, these results suggest that the tail domain interferes with tomosyn complex formation upon its direct binding to the VLD, and thereby reduces the inhibition of SNARE complex formation.

Direct Binding of the Tail Domain to the N-terminal WD40 Repeats—We next compared the activity of full-length tomosyn to inhibit SNARE complex formation with those of Tail-VLD and VLD. The SNARE proteins were reacted in the absence or presence of MBP-fused full-length tomosyn (MBP-

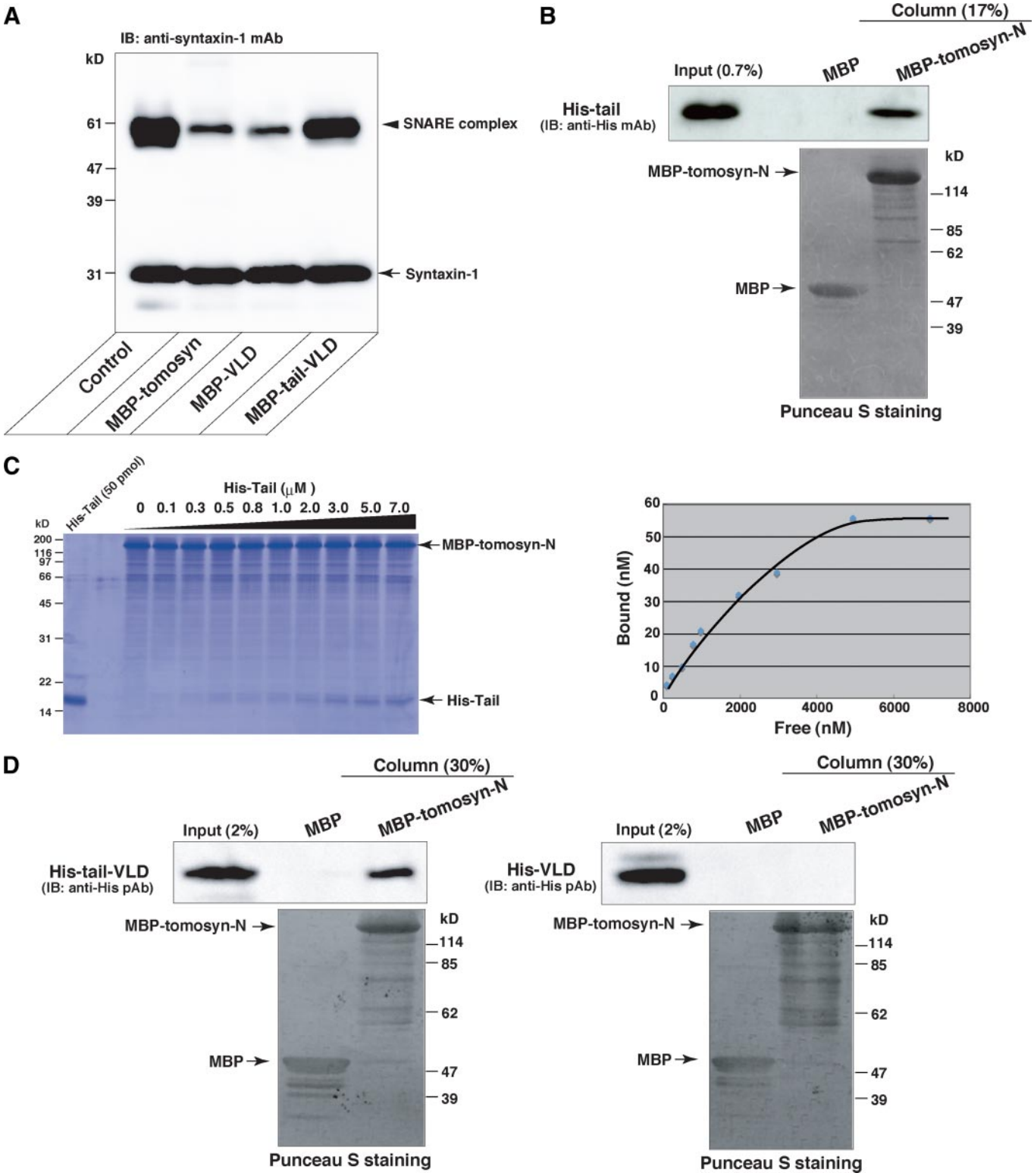

FIGURE 5. **Direct binding of the tail domain to the N-terminal WD40 repeats.** *A*, potent inhibition of the SNARE complex formation by full-length tomosyn. 0.5 μM syntaxin-1, 0.5 μM SNAP-25, and 0.5 μM VAMP-2 were reacted in the presence or absence of 1 μM MBP-tomosyn, 1 μM MBP-VLD, or 1 μM MBP-tail-VLD. The samples were solubilized in SDS sample buffer at room temperature for 10 min, and subjected to SDS-PAGE followed by immunoblotting (*IB*) with the anti-syntaxin-1 mAb. *B*, direct binding of the tail domian to the N-terminal WD40 repeats. MBP-tomosyn-N and MBP alone were immobilized on amylose resins, respectively, and then the resins were incubated with His-tail. After extensive wash of the resins, the bound proteins were eluted by boiling in SDS sample buffer. 0.7% of Input and 17% of the eluted proteins were subjected to SDS-PAGE followed by immunoblotting (*IB*) with the anti-His mAb. *C*, quantitative analysis of the binding of the tail domian to the N-terminal WD40 repeats. 130 pmol of MBP-tomosyn-N were immobilized on amylose resin, and incubated with various concentrations of His-tail. After extensive wash of the resin, the bound proteins were eluted by boiling in the SDS sample buffer and subjected to SDS-PAGE followed by Coomassie Brilliant Blue staining. The bound His-tail was quantified in the *right panel*. *D*, binding of Tail-VLD but not VLD to Tomosyn-N. MBP-tomosyn-N or MBP was immobilized on amylose resin and incubated with His-tail-VLD or His-VLD. After extensive wash of the resins, the bound proteins were eluted by boiling in SDS sample buffer. 2% of Input and 30% of the eluted proteins were subjected to SDS-PAGE, followed by immunoblotting with the anti-His polyclonal antibody.

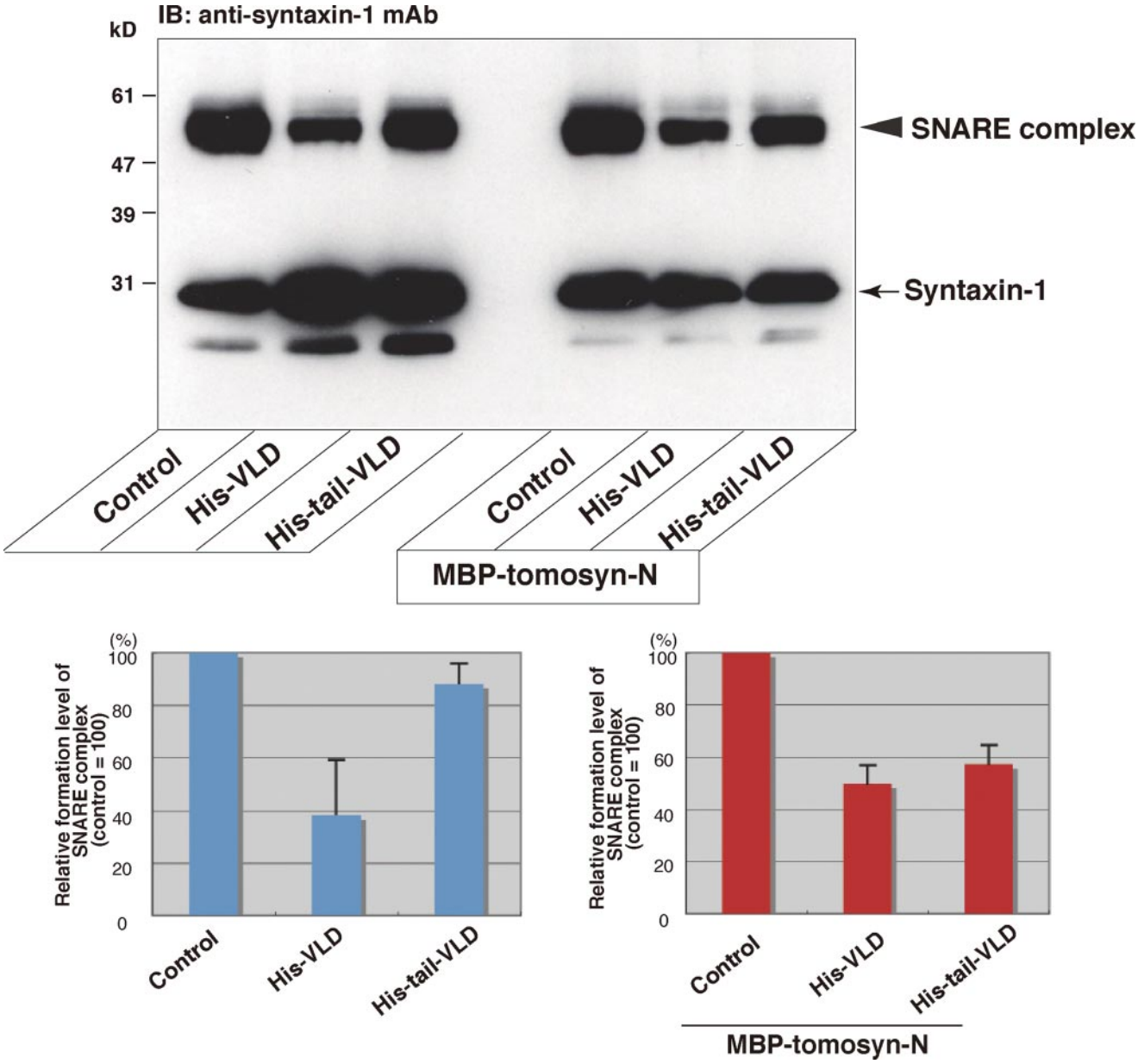

FIGURE 6. **Role of the binding of the tail domain to the N-terminal WD40 repeats in inhibition of the SNARE complex formation.** In the *left half* of the *upper panel*, 0.25 μM syntaxin-1, 0.25 μM SNAP-25, and 0.25 μM VAMP-2 were reacted in the presence or absence of 0.25 μM His-VLD or 0.25 μM His-tail-VLD, and the samples were subjected to SDS-PAGE followed by immunoblotting (*IB*) with the anti-syntaxin-1 mAb. In the *right half* of the *upper panel*, 0.5 μM MBP-tomosyn-N was preincubated with 0.25 μM His-VLD or 0.25 μM His-tail-VLD. 0.25 μM syntaxin-1, 0.25 μM SNAP-25, and 0.25 μM VAMP-2 were reacted in the presence of the preincubated mixtures of MBP-tomosyn-N and His-VLD or His-tail-VLD, or MBP-tomosyn-N alone, and the samples were solubilized in the SDS sample buffer at room temperature for 10 min, and subjected to SDS-PAGE followed by immunoblotting with the anti-syntaxin-1 mAb. Quantification of the relative formation of the SNARE complex is shown in the *lower panels*. The result shown is representative of three independent experiments. *Error bars* represent S.D.

tomosyn), MBP-tail-VLD, or MBP-VLD, and then SNARE complex formation was examined by immunoblotting with the anti-syntaxin-1 mAb. MBP-tomosyn potently inhibited SNARE complex formation as much as MBP-VLD did (Fig. 5*A*). The fact that despite the existence of both the tail domain and the VLD, that full-length tomosyn potently inhibited SNARE complex formation prompted us to examine whether the N-terminal WD40 repeats bound the tail domain. An MBP-fused large N-terminal fragment of tomosyn encompassing the WD40 repeats but lacking the tail domain and the VLD (MBP-tomosyn-N) as shown in Fig. 1*A* and MBP alone were immobilized on amylose resins, respectively, and then the resins were incubated with His-tail. Specific binding of His-tail to MBP-tomosyn-N was detected by immunoblotting with the anti-His polyclonal antibody (Fig. 5*B*). Next, we examined the affinities of the interactions of the tail domain with the N-terminal WD40 repeats and the VLD quantitatively. Equal amounts of MBP-tomosyn-N and GST-VLD were immobilized on amylose resin and glutathione-Sepharose, respectively, and incubated with various concentrations of His-tail. The binding of His-tail to MBP-tomosyn-N was detected on the Coomassie Brilliant Blue gel (Fig. 5*C*). The binding was saturated at ~5000 nM free

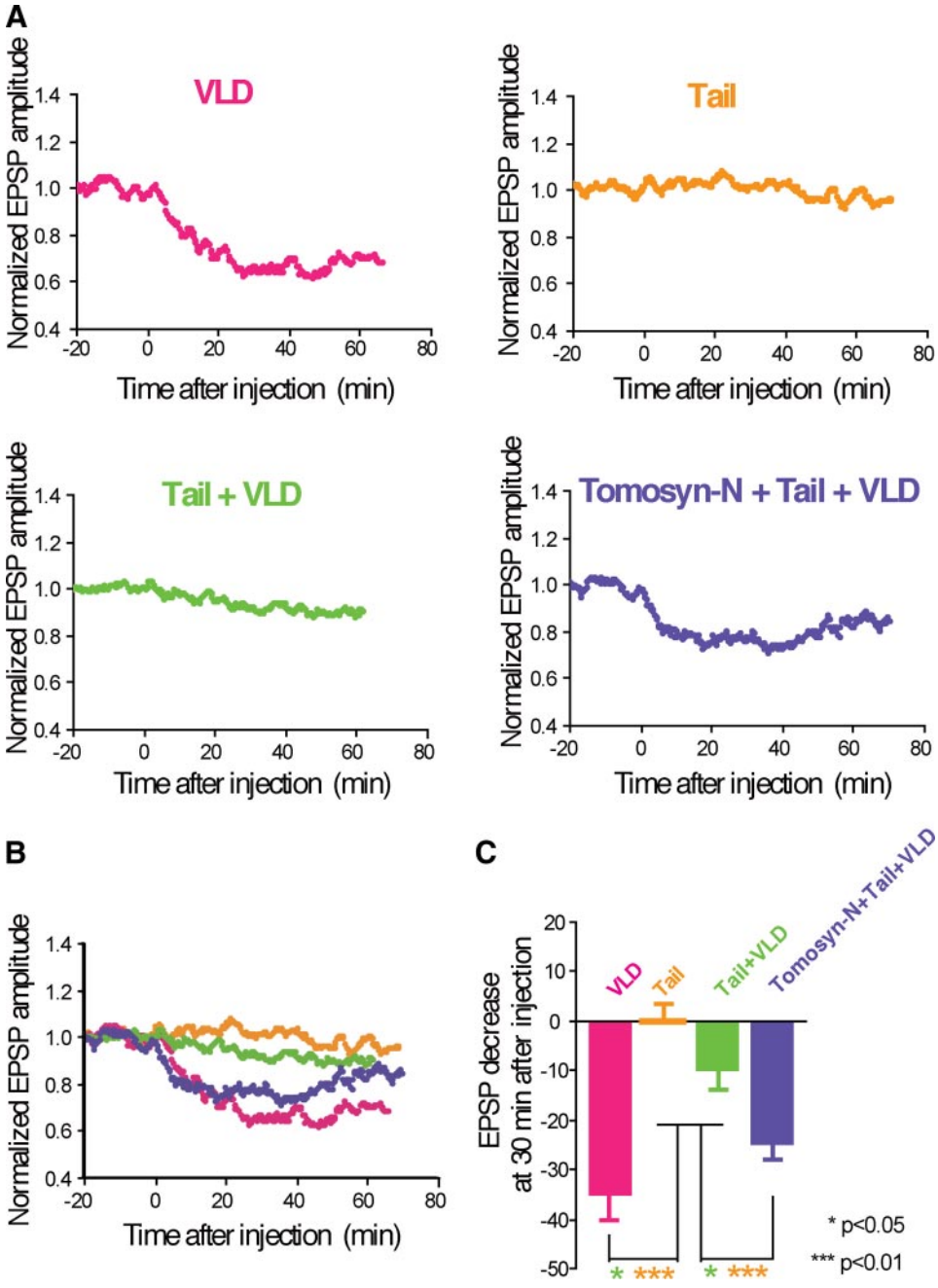

FIGURE 7. **Roles of the reciprocal bindings of the tail domain to the N-terminal WD40 repeats and the VLD in regulation of neurotransmitter release.** *A*, modulation of inhibition of synaptic transmission upon the bindings of the tail domain to the N-terminal WD40 repeats and the VLD. Indicated combinations of tomosyn fragments were microinjected into the cell bodies of SCG neurons at time = 0 (100 μM each in the pipette). EPSP amplitudes measured every 10 s were normalized and averaged (n = 4 or 8). The mean values smoothed by an eight-point moving average algorithm are plotted. *VLD*, MBP-VLD (a repetition of Fig. 1*B*); *Tail*, His-tail; *Tail + VLD*, the mixture of His-tail and MBP-VLD; *Tomosyn-N + Tail + VLD*, the mixture of MBP-tomosyn-N, His-tail, and MBP-VLD. *B*, merged graph. The smoothed mean values shown in *A* were merged into a single graph. *C*, decrease in EPSP amplitude at 30 min after microinjection of the tomosyn fragments. *Error bars* represent S.E.

His-tail. By contrast, the binding of His-tail to GST-VLD was not detected by Coomassie Brilliant Blue staining but detected by immunoblotting with the anti-His mAb under the same condition as the binding of His-tail to MBP-tomosyn-N was detected by Coomassie Brilliant Blue staining (supplemental Fig. S5*A*). These results indicate that the affinity of the tail domain to the N-terminal WD40 repeats is stronger than that to the VLD. To further confirm these observations, we examined whether the N-terminal WD40 repeats interfered with binding of the tail domain to the VLD. GST-VLD immobilized on glutathione-Sepharose was incubated with the His-tail in the presence of various amounts of MBP-tomosyn-N. MBP-tomosyn-N reduced the binding of His-tail to GST-VLD in a dose-dependent manner (supplemental Fig. S5*B*). In addition, we detected binding of Tail-VLD but not VLD to tomosyn-N by *in vitro* assay using the purified recombinant proteins (Fig. 5*D*) and co-immunoprecipitation assay using HEK293 cells (supplemental Fig. S4*B*). These results also support that the tail domain binds the N-terminal WD40 repeats and that the affinity of the tail domain to the N-terminal WD40 repeats is stronger than that to the VLD.

Role of the Binding of the Tail Domain to the N-terminal WD40 Repeats in Regulation of the SNARE Complex Formation—Based on the above results, we reasoned that the N-terminal WD40 repeats had an ability to displace the tail domain from the VLD, leading to the VLD-mediated potent inhibition of SNARE complex formation. To test this, we examined the effect of the binding of the N-terminal WD40 repeats to Tail-VLD on inhibition of SNARE complex formation. The SNARE proteins were reacted in the presence or absence of His-VLD alone, His-tail-VLD alone, MBP-tomosyn-N alone, the mixture of MBP-tomosyn-N and His-tail-VLD, or the mixture of MBP-tomosyn-N and His-VLD, and SNARE complex formation was detected by immunoblotting with the anti-syntaxin-1 mAb. Consistent with the results using MBP-VLD and MBP-tail-VLD as shown in Fig. 2, His-tail-VLD moderately inhibited SNARE complex formation relative to His-VLD (Fig. 6). By contrast, the mixture of MBP-tomosyn-N and His-tail-VLD potently inhibited SNARE complex formation as much as His-VLD. These results indicate that the N-terminal WD40 repeats displaces the tail domain from the VLD, leading to the VLD-mediated potent inhibition of the SNARE complex formation.

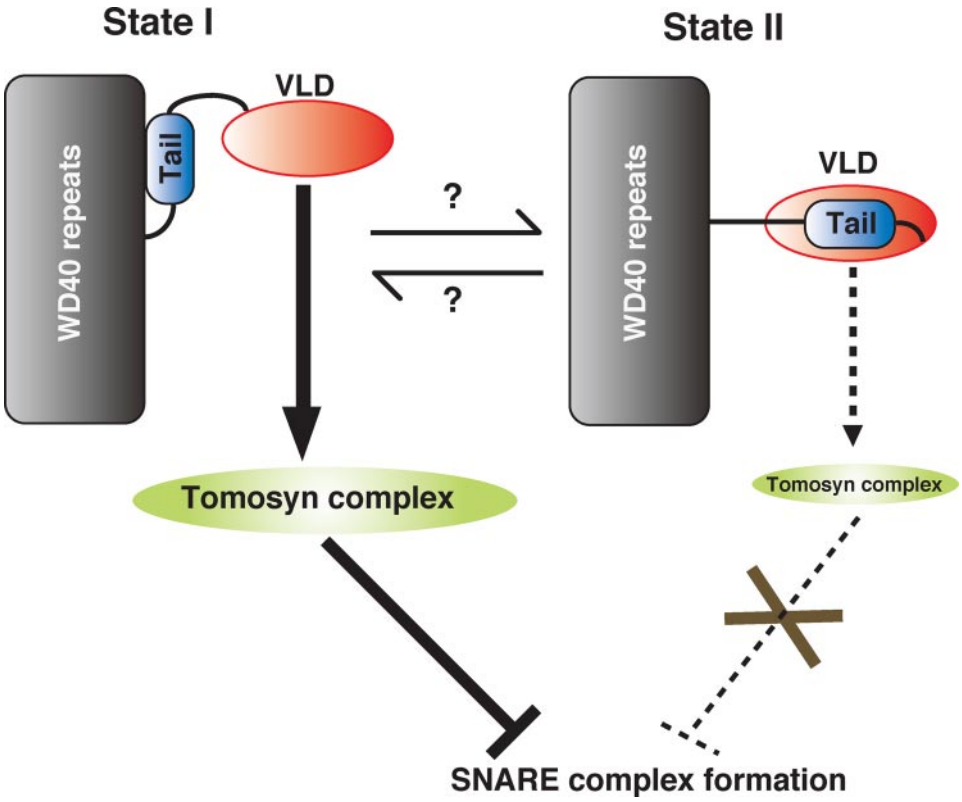

FIGURE 8. **A model of regulation of the inhibitory activity of tomosyn upon the tail domain bindings.** In state I, tomosyn exposes the VLD upon binding of the tail domain to the N-terminal WD40 repeats, leading to efficient tomosyn complex formation. Eventually, tomosyn potently inhibits SNARE complex formation. In state II, VLD is masked by the tail domain, leading to less formation of the tomosyn complex. Eventually, tomosyn does not inhibit the SNARE complex formation.

Roles of the Reciprocal Bindings of the Tail Domain to the N-terminal WD40 Repeats and the VLD in Regulation of Neurotransmitter Release—We electrophysiologically characterized the interactions of the tail domain with the VLD and the N-terminal WD40 repeats. Various combinations of tomosyn fragments were microinjected into SCG neurons and acetylcholine release was monitored by recording EPSPs. Whereas microinjection of MBP-VLD alone potently inhibited acetylcholine release, microinjection of the mixture of His-tail and MBP-VLD slightly inhibited acetylcholine release (Fig. 7). Microinjection of His-tail alone had no influence on acetylcholine release. These results indicate that the inhibitory activity of MBP-VLD is inhibited by its binding to the His-tail, and are in good agreement with the biochemical results that the inhibitory activity of the VLD on SNARE complex formation is reduced by its binding to the tail domain as shown in Fig. 4*C*. Moreover, microinjection of the mixture of MBP-tomosyn-N, His-tail, and MBP-VLD inhibited acetylcholine release more than microinjection of the mixture of His-tail and MBP-VLD, indicating that binding of MBP-tomosyn-N to His-tail displaces His-tail from MBP-VLD, resulting in restoration of the inhibitory activity of MBP-VLD. These results are in good agreement with the biochemical results that the binding of the N-terminal WD40 repeats to the tail domain restores the inhibitory activity of the VLD on SNARE complex formation as shown in Fig. 6. Taken together, these results indicate that the reciprocal intramolecular interactions of the tail domain with the VLD and N-terminal WD40 repeats control the inhibitory activity of tomosyn on the SNARE complex formation, leading to regulation of neurotransmitter release. We recently reported that the N-terminal WD40 repeats inhibit neurotransmitter release through oligomerization of the SNARE complex (26). Consistent with this report, microinjection of MBP-tomosyn-N alone potently inhibited acetylcholine release (supplemental Fig. S6). The mixture of MBP-tomosyn-N, His-tail, and MBP-VLD inhibited acetylcholine release less than MBP-tomosyn-N alone. Therefore, the inhibitory activity of the N-terminal WD40 repeats may be modulated via its binding to the tail domain.

DISCUSSION

In this study, we biochemically and electrophysiologically demonstrated that the tail domain of tomosyn acts as a regulatory domain for the VLD. The tail domain directly binds to the VLD, and thereby represses the VLD-mediated inhibition of SNARE complex formation. Binding of the tail domain to the N-terminal WD40 repeats restores the repressed VLD-mediated inhibition of SNARE complex formation. Tomosyn might be in a state of equilibrium between two conformational states upon the tail domain binding (Fig. 8). In one conformational state (state I), the tail domain binds the N-terminal WD40 repeats, leading to exposure of the VLD. The exposed VLD efficiently forms the tomosyn complex with t-SNAREs, resulting in the potent inhibition of SNARE complex formation. In the other conformational state (state II), the tail domain masks the VLD and thereby blocks tomosyn complex formation, resulting in loss of the inhibition of the SNARE complex formation. In support of the idea of equilibrium, full-length tomosyn moderately inhibited SNARE complex formation relative to the VLD alone in a time-dependent manner, suggesting that full-length tomosyn exists in both forms (data not shown). MBP-tail-VLD but not MBP-VLD shows the vague migration on the native gel (Fig. 3 and supplemental Fig. S3), suggesting that the surface charge of MBP-tail-VLD is variable presumably due to both binding and dissociation between the tail domain and the VLD. These results provide other lines of evidence that tomosyn is in a state of equilibrium between the two conformational states upon the tail domain binding. The binding affinity of the tail domain to the N-terminal WD40 repeats was stronger than that to the VLD. Despite the existence of both the tail domain and the VLD in full-length tomosyn, full-length tomosyn inhibited SNARE complex formation more than Tail-VLD. Therefore, state I is

probably a dominant state. What drives the conformational change from state I to state II? We previously reported that protein kinase A phosphorylates tomosyn, resulting in reducing the binding of the VLD to syntaxin-1 (25). Therefore, protein kinase A may be a possible regulator to drive the conformational change. Physiological meaning of the structural regulation of tomosyn upon tail binding still remains elusive. We recently generated tomosyn-deficient mice, characterized them electrophysiologically, and revealed that the tomosyn-deficient mice lacked short-term potentiation (26). Therefore, the structural regulation of tomosyn may be important for short-term memory. We also reported that the N-terminal WD40 repeats have an activity to inhibit neurotransmitter release through oligomerization of the SNARE complex (26). Given that microinjection of a mixture of MBP-tomosyn-N, His-tail, and MBP-VLD into the SCG neurons inhibited acetylcholine release less than microinjection of MBP-tomosyn-N alone, binding of the tail domain to the N-terminal WD40 repeats might modulate the activity of the N-terminal WD40 repeats to oligomerize the SNARE complex. Further studies will be needed for understanding the regulation of the conformational change of tomosyn.

The N-terminal WD40 repeats of tomosyn shares similarity to the *Drosophila* tumor suppressor D-Lgl, its mammalian homologues M-Lgl1 and M-Lgl2, and yeast proteins Sro7p and Sro77p, which play important roles in polarized exocytosis by regulating SNARE function on the plasma membrane in *Drosophila* neuroblasts, mammalian epithelial cells, and yeast, respectively (13). However, only tomosyn, Sro7, and Sro77 have tail domains and C-terminal VAMP-like domains, raising the possibility that structural regulation of those may be evolutionally conserved (27). A recent structural study of Sro7 revealed that the tail domain of Sro7 binds the bottom surface of the N-terminal WD40 repeats, in good agreement with our results of direct binding of the tail domain of tomosyn to the N-terminal WD40 repeats (14). The study also suggested that binding of the tail domain to the N-terminal WD40 repeats causes a conformational change of Sro7, and interferes with interaction of the N-terminal WD40 repeats with Sec9, a yeast counterpart of SNAP-25, leading to regulation of the inhibitory activity of Sro7 on SNARE complex formation (14). These are inconsistent with our present finding that binding of the tail domain to the N-terminal WD40 repeats leads to exposure of the VLD, resulting in inhibition of SNARE complex formation. However, the solved structure of Sro7 lacks the C-terminal domain corresponding to the VLD. Therefore, involvement of activity of the VLD in the conformational change of Sro7 upon tail domain binding remains elusive, as mentioned recently (27). Considering the evolutionally conserved molecular structure of Sro7, Sro7 may use the binding of the tail domain to the N-terminal WD40 repeats to regulate the activity of its VLD in the same manner as tomosyn. Future structural studies of full-length tomosyn and full-length Sro7 will elucidate these concerns. In summary, we propose here a structural regulation of the inhibitory activity of the VLD of tomosyn upon tail domain bindings, which plays an important role in controlling SNARE complex formation.

REFERENCES

1. Südhof, T. C. (2004) *Annu. Rev. Neurosci.* **27,** 509–547
2. Sutton, R. B., Fasshauer, D., Jahn, R., and Brunger, A. T. (1998) *Nature* **395,** 347–353
3. Weber, T., Zemelman, B. V., McNew, J. A., Westermann, B., Gmachl, M., Parlati, F., Söllner, T. H., and Rothman, J. E. (1998) *Cell* **92,** 759–772
4. Jahn, R., and Scheller, R. H. (2006) *Nat. Rev. Mol. Cell Biol.* **7,** 631–643
5. Rizo, J., and Rosenmund, C. (2008) *Nat. Struct. Mol. Biol.* **15,** 665–674
6. Trimble, W. S., Cowan, D. M., and Scheller, R. H. (1988) *Proc. Natl. Acad. Sci. U. S. A.* **85,** 4538–4542
7. Bennett, M. K., Calakos, N., and Scheller, R. H. (1992) *Science* **257,** 255–259
8. Söllner, T., Bennett, M. K., Whiteheart, S. W., Scheller, R. H., and Rothman, J. E. (1993) *Cell* **75,** 409–418
9. Chen, Y. A., and Scheller, R. H. (2001) *Nat. Rev. Mol. Cell Biol.* **2,** 98–106
10. Fujita, Y., Shirataki, H., Sakisaka, T., Asakura, T., Ohya, T., Kotani, H., Yokoyama, S., Nishioka, H., Matsuura, Y., Mizoguchi, A., Scheller, R. H., and Takai, Y. (1998) *Neuron* **20,** 905–915
11. Pobbati, A. V., Razeto, A., Boddener, M., Becker, S., and Fasshauer, D. (2004) *J. Biol. Chem.* **279,** 47192–47200
12. Lehman, K., Rossi, G., Adamo, J. E., and Brennwald, P. (1999) *J. Cell Biol.* **146,** 125–140
13. Wirtz-Peitz, F., and Knoblich, J. A. (2006) *Trends Cell Biol.* **16,** 234–241
14. Hattendorf, D. A., Andreeva, A., Gangar, A., Brennwald, P. J., and Weis, W. I. (2007) *Nature* **446,** 567–571
15. Gracheva, E. O., Burdina, A. O., Holgado, A. M., Berthelot-Grosjean, M., Ackley, B. D., Hadwiger, G., Nonet, M. L., Weimer, R. M., and Richmond, J. E. (2006) *PLoS Biol.* **4,** e261
16. McEwen, J. M., Madison, J. M., Dybbs, M., and Kaplan, J. M. (2006) *Neuron* **51,** 303–315
17. Constable, J. R., Graham, M. E., Morgan, A., and Burgoyne, R. D. (2005) *J. Biol. Chem.* **280,** 31615–31623
18. Yizhar, O., Lipstein, N., Gladycheva, S. E., Matti, U., Ernst, S. A., Rettig, J., Stuenkel, E. L., and Ashery, U. (2007) *J. Neurochem.* **103,** 604–616
19. Yasumi, M., Sakisaka, T., Hoshino, T., Kimura, T., Sakamoto, Y., Yamanaka, T., Ohno, S., and Takai, Y. (2005) *J. Biol. Chem.* **280,** 6761–6765
20. Fasshauer, D., Otto, H., Eliason, W. K., Jahn, R., and Brünger, A. T. (1997) *J. Biol. Chem.* **272,** 28036–28041
21. Mochida, S., Nonomura, Y., and Kobayashi, H. (1994) *Microsc. Res. Tech.* **29,** 94–102
22. Mochida, S., Sheng, Z. H., Baker, C., Kobayashi, H., and Catterall, W. A. (1996) *Neuron* **17,** 781–788
23. Hayashi, T., McMahon, H., Yamasaki, S., Binz, T., Hata, Y., Südhof, T. C., and Niemann, H. (1994) *EMBO J.* **13,** 5051–5061
24. Ma, H., and Mochida, S. (2007) *Neurosci. Res.* **57,** 491–498
25. Baba, T., Sakisaka, T., Mochida, S., and Takai, Y. (2005) *J. Cell Biol.* **170,** 1113–1125
26. Sakisaka, T., Yamamoto, Y., Mochida, S., Nakamura, M., Nishikawa, K., Ishizaki, H., Okamoto-Tanaka, M., Miyoshi, J., Fujiyoshi, Y., Manabe, T., and Takai, Y. (2008) *J. Cell Biol.* **183,** 323–337
27. Fasshauer, D., and Jahn, R. (2007) *Nat. Struct. Mol. Biol.* **14,** 360–362